Permanent Magnets in Use Today

By Fred E. Luborsky, General Electric Research and Development Center, Building 81, Room E113, Schenectady, NY 12345

Abstract

The present status of our concepts as to the origin of the structure and behavior of permanent magnet materials now in use is discussed. It is shown that domain theory can at least qualitatively explain the properties of all these permanent magnet materials. In some cases quantitative agreement between theory and observed properties has been achieved, e.g., with elongated single-domain particle magnets and with iron and iron-cobalt whiskers smaller than about 1000 Å in diameter. Such cases are shown to improve our understanding of both the structure and properties of the more complex Alnico alloys.

Introduction

The many varieties of magnets in use today may be classified according to their metallurgical structures into four categories:

(1) Magnet steels,

(2) Precipitation-hardened alloys,

(3) Order-hardened alloys, and

(4) Fine-particle magnets.

In terms of our understanding of the origin of their magnetic behavior, only two categories are necessary:

(1) the inclusion hardened alloys represented by the magnet steels and

(2) the fine-particle magnets.

These include both synthetic structures such as Lodex® or ferrites as well as metallurgical structures, for example, the Alnicos or CoPt.

Inclusion-Hardened Magnets

The properties of the magnet steels have been described by many authors.[1] Their coercive force H_{ci} originates from the energy barriers to domain boundary movement. These barriers are due to the combined effects of nonmagnetic inclusions, internal strains, lattice defects, inhomogeneities, and holes. The specific compositions and processing of each of the magnet steels are so arranged as to optimize the combined effect of these barriers to domain boundary motion to achieve the maximum H_{ci}.

Fine-Particle Magnets

Alnico

The basic Alnico alloys develop their magnetic phase through a spinodal decomposition[2] of the high-temperature homogeneous α phase into the FeCo-rich α and the NiAl-rich α' phases. In the initial stages a discrete precipitate does not form; rather, the two phases develop by a gradual fluctuation in composition. Theory predicts[3] that the resulting structures will be periodic in nature and crystallographically oriented. The permanent magnet microstructures in Figure 1 show both of these characteristics. The effect of a magnetic field is to enhance compositional waves parallel to the applied field, suppressing transverse waves.

Typical results are shown in Figure 1a, 1c, and 1d. The wavelength is a characteristic of the undercooling $T_s - T$, where T_s is the temperature of the boundary between the α and α' phases. The wavelength decreases with increasing undercooling.

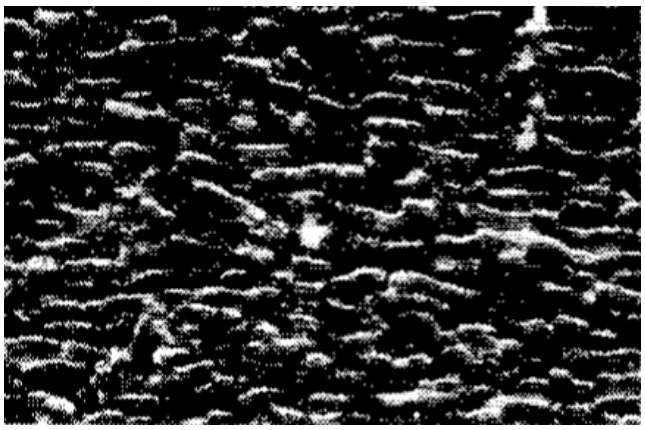

Figure 1a — Magnet microstructures resulting from spinodal decomposition. Alnico 5 micrograph of replica parallel to field treating direction, J. de Jong, J. Smeets, and H. Haanstra; Journal of Applied Physics 29, pp. 297 (1958)

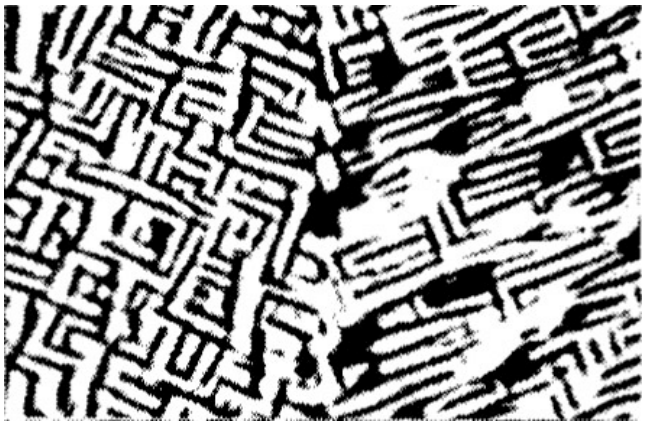

Figure 1b — Magnet microstructures resulting from spinodal decomposition. Alnico 3 polished and etched surface seen by reflected light, A. Bradley; Journal Iron and Steel Institute 168, 233 (1951). Alnico 3 shows two differently oriented crystals. Magnification marker corresponds to 5 μ

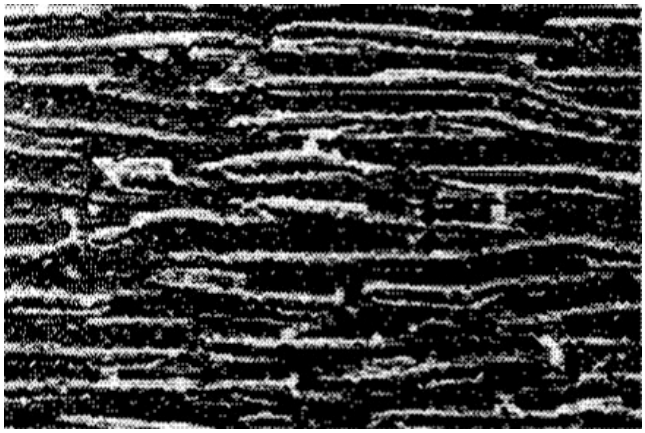

Figure 1c — Magnet microstructures resulting from spinodal decomposition. Alnico 8 replica parallel. Magnification marker corresponds to 0.1 μ

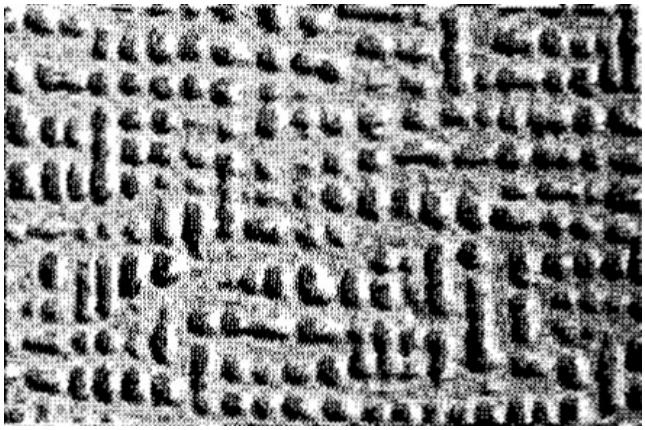

Figure 1d — Magnet microstructures resulting from spinodal decomposition. Alnico 8 replica perpendicular to the field-treating direction. Reference same as 1a.

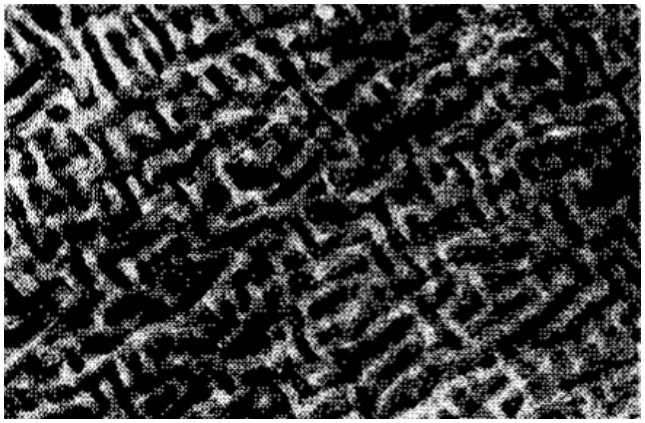

Figure 1e — Magnet microstructures resulting from spinodal decomposition. Cunife transmission micrographs (P. Tufton, thesis, University of Cambridge, 1963). Magnification marker corresponds to 0.1 μ

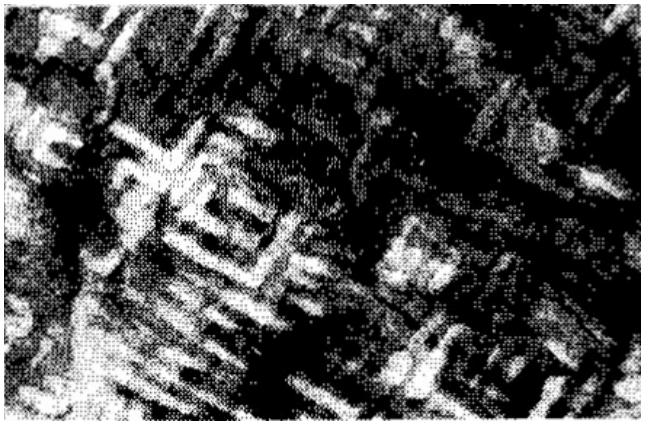

Figure 1f — Magnet microstructures resulting from spinodal decomposition. Cunico transmission micrographs (P. Tufton, thesis, University of Cambridge, 1963). Magnification marker corresponds to 0.1 μ

Note: Figures 1a to 1 f were all aged to near optimum magnetic properties.

The effectiveness of the field in restricting the growth of the perpendicular compositional waves depends on the difference in magnetization between the crest and the trough of a concentration wave. The greatest effect of the field will thus be obtained when the derivative of the saturation magnetization M_8 with respect to composition is large. This occurs when decomposition is carried out near the Curie temperature T_c and when T_c is near T_s. The lack of orientation effects by a magnetic field in the Alni alloys where T_s is not near T_c and the strong effect of the magnetic field in the Alnico alloys where T_s is near T_c (see Table 1) is accounted for by the theory. The contribution of transverse waves causes a periodic modulation in thickness of the rods. This rough peanut-like shape is typical of the Alnico 5 alloys as shown in Figure 1. On the other hand, in the Alnico 8 alloy this modulation in thickness is not present and may account[4] for 'a good part of the increased H_{ci} ob-

served in these alloys over Alnico 5. The smoother shape comes about because the magnetic annealing can be carried out at a small degree of undercooling, since T_s and T_c are close together. This spinodal model is consistent with all of the observed experimental facts, namely x-ray line broadening, periodicity of the microstructure, the effect of magnetic field on the aging, crystallographic orientation of the structure, and the relation between T_c, T_s, and magnetic-field treatment temperature.

From the theory, it would seem reasonable to expect that the most uniform elongated shape of the magnetic phase, and consequently the ideal magnetic properties, would be achieved when Alnico 5 is isothermally treated in a magnetic field rather than given the continuous cooling treatment commonly used. During a continuous cooling the alloy must inevitably pass temperature regions where the effectiveness of the field in impairing the growth of the transverse waves is poor. This cooling treatment may also contribute to the imperfect morphology observed in Alnico 5. In the case of Alnico 8, isothermal treatment does give properties superior to a slow cooling treatment. Isothermal treatment of usable sizes of Alnico 5 is not beneficial because of the very narrow temperature region required,[5] on the order of 1°C. The final aging at ~600°C, required to develop the best properties in Alnico, acts by enriching the strongly magnetic α phase with FeCo and the weakly magnetic α' phase with NiAl. This enrichment is expected from the phase diagram.

The best properties of the Alnico alloys require development of the [100] crystal texture so that the magnetic field is along a [100] axis in all crystals in order to properly influence the spinodal decomposition as discussed above. For Alnico 5 this texture is quite easy to obtain by a variety of techniques,[6] but for alloys with more than a few percent Ti, for example the Alnico 8 alloy, columnar crystallization has been much more difficult to achieve. Samples were made[6] in the laboratory by carefully controlling the melt purity and the atmosphere. Recently it was discovered[6] that the addition of S or Se greatly facilitates columnar crystallization, probably by a simple slagging action to remove oxides or inclusions which otherwise would promote nucleation of grains ahead of the growing crystal. More recently[7] Ce, Pb, Cd, and Bi have produced the same effect.

Cunife and Cunico

The coercive force of these alloys can be accounted for by the shape anisotropy of FeNi- or CoNi-rich magnetic regions in a copper-rich nonmagnetic matrix. This conclusion is based on observations of microstructures, temperature dependence of properties, and compositional effects as in Figure 2. Cold working of Cunife produces a crystallographic texture which is enhanced by subsequent annealing, but no significant texture can be developed in Cunico. Since spinodal decomposition occurs along definite crystallographic planes, as shown in the micrographs in Figure 1, the crystal texture in Cunife gives rise to magnetic texture. Aging in a magnetic field has essentially no influence on these alloys because T_c is too far below T_s as shown in Table 1.

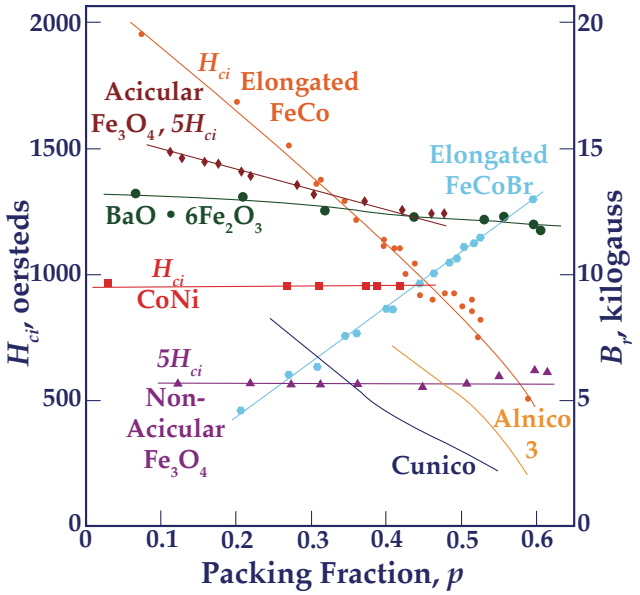

Figure 2 — Effect of packing of magnetic phase on intrinsic coercive force for materials with predominantly crystal anisotropy BaO 6Fe20a, CoNi, and non acicular FeaO, particles; and with predominantly shape anisotropy-elongated FeCo particles and a series of Alnico 3 and Cunico alloys. Acicular FeaO particles show contributions from both shape and crystal anisotropy.

Table 1 — Decomposition and Curie temperatures of magnetic alloys decomposing spinodally

Designation	Composition (weight %)						T_c (°C)	T_s (°C)	Effect of Field During Aging
	Al	Ni	Co	Cu	other	Fe			
—	—	23	—	—	77 Au	—	Paramagnetic	850	No
Cunico	—	20	30	50	—	—	885	1095	No
Cunife	—	20	—	60	—	20	410	980	No
	—	30	—	50	—	20	500	970	No
Alnico 3	12	25	—	—	—	63	740	950	No
Alnico 5	8	14	24	3	—	51	890	850	Yes
Alcomax IV	8	14	24	3	2 Nb	49	860	<850	Yes
Alnico 8	7	14.5	35	5	5 Ti	33.5	860	845	Yes

Cobalt Platinum

In the case of CoPt the high H_{ci} may be attributed to the high crystal anisotropy constant K of the face centered slightly tetragonal single-domain-ordered regions. In support of this, for example, cobalt platinum made as a fine single-domain powder from the hydrogen reduction of $CoPtCN_4$ has properties comparable to the cast material and yet is crystallographically completely ordered. The large value of B_r/B_{is} in the random state of 0.86 suggests a cubic magneto-crystalline anisotropy as the dominant contribution to H_{ci}.

Ferrite Magnets

The magnetic oxides of the magnetoplumbite type, $BaO{\bullet}6Fe_2O_3$ and $SrO{\bullet}6Fe_2O_3$, are made by firing the suitable oxides, grinding to single-domain size, pressing in a magnetic field, and then sintering. Their high H_{ci} is derived from their crystal anisotropy as indicated from the relation between K/M_s and H_{ci} as a function of temperature,[8] the effect of particle packing as shown in Figure 2, and the appearance of the microstructure. The H_{ci} for the strontium ferrite, a major component in one of the newer ferrites, is somewhat higher than for the barium ferrite due to a slightly higher K as given in Table 2. Recently values of H_{ci} as high as 11,300 Oe have been reported[9] in modified strontium ferrite materials. Additions of minor amounts of various materials are used to isolate the single-domain grains, promote compacting and sintering, and aid in grain alignment. The specific role of each of these minor constituents is usually not clear.

Elongated-Particle Magnets

Elongated particles of single-domain size are prepared by a unique series of steps starting with electrodeposition of FeCo into mercury. The final magnet structure consists of elongated particles of FeCo isolated from each other by a monolayer of Sb and imbedded in a PbSb matrix.[10] The high H_{ci} can be accounted for quantitatively[10] on the basis of the shape anisotropy of the individual particles plus a small crystal anisotropy contribution. The domain structures observed on finished magnets are the same as observed on Alnico. These have been called[11] interaction domains and are the result of the coupling between many millions of particles so that their magnetization vectors act together.

Magnetization Reversal Processes

The mechanism of magnetization reversal and the relative contributions of shape or crystal anisotropies are elucidated through studies of various magnetic properties, e.g., K vs temperature, H_{ci} and H_{ci} vs diameter, packing, and temperature, rotational hysteresis, and angular variation of properties.

Magnetic materials with crystal anisotropy as the dominant contribution to their H_{ci} show a remarkably good

correlation between calculated and observed H_{ci}, as shown in Table 2. The agreement is not quantitative because the specific method of preparation of each material may produce defects, strains, non-spherical particles, changes in crystal structure or changes in oxidation state. These changes, which may be modified by annealing, result in complicated contributions to H_{ci}, B_r, and B_{is}. In general the maximum reported H_{ci} is 30% to 70% of the theoretical value. In some cases the discrepancy is understood, e.g., the high H_{ci} of the Fe powder is due to a significant shape anisotropy contribution while crystal imperfections in general are the dominant factor contributing to low-energy domain nucleation and hence low H_{ci}.

In the case of magnets where shape anisotropy is the dominant contribution to the H_{ci}, e.g., in Alnico and in Lodex, the magnetic properties are adequately described[10] by the non-symmetric fanning model in a chain of spheres, although the crystal anisotropy of the <111>-oriented particles in Lodex and slight branching and bridging in both Alnico and Lodex playa role in modifying the simple theoretical picture.[4] Fanning is a lower energy process than coherent rotation, but it has been shown[12] from experiments on almost perfect whiskers of Fe and FeCo alloys that the particle shape perfection strongly influences the mode of magnetization reversal. The properties of whiskers with diameters between 200 and 1000 Å could be accounted for quantitatively on the basis of their shape anisotropy using a curling mode of reversal. More recent experiments on Ni whiskers gave the same properties as found for Fe and FeCo when the different values of M_s and exchange constant are considered.

Table 2 — Crystal Anisotropy and Particle Coercive Force at Room Temperature

Material	Crystal Structure	Easy Axis	Anisotropy constant (erg/cm^3) x 10^{-6}		M_s (emu/cm^3)	Maximum H_{ci} (Oe)		
			K_1	K_2		Calc.[a]	Reported[b]	Reference
MnAl	Tetragonal	c	-10		495	~40,000	6,000	c
MnBi	Hexagon	c	8.9	2.7	620	37,000	12,000	d
$SrO \cdot 6Fe_2O_3$	Hexagon	c	3.7		365	20,000	11,300	e
$BaO \cdot 6Fe_2O_3$	Hexagon	c	3.3		380	17,000	5,400	f
$PbO \cdot 6Fe_2O_3$	Hexagon	c	2.2	0.03	320	14,000	3,500	g
Co	Hexagon	c	4.0	2.0	1,400	4,100	2,100 [r]	h
$CoFe_2O_4$	Cubic	[100]	2.5		425	3,750	2,080 [r]	i
Fe_4N	Cubic	[100]	~6		1,390	~2,750	580 [r]	j
Fe_3C	Orthorh.	c	1.18		990	1,150	700 [r]	k
Mn_2Sb	Tetragonal	c	0.27		230	1,100	280 [r]	l
$CuFe_2O_4$	Cubic	[111]	-0.060		135	380	530 [r]	m
$NiFe_2O_4$	Cubic	[111]	-0.05	-0.20	270	370	280 [r]	n
Fe_3O_4	Cubic	[111]	-0.11	-0.28	480	360	140 [r]	o
Te	Cubic	[100]	0.47	0	1700	175	1,000 [r]	p
Ni	Cubic	[111]	-0.049	-0.042	480	110	69 [r]	q
γFe_2O_3	Cubic	[100]	0.047		400	75	90 [r]	r
$MnFe_2O_4$	Cubic	[111]	-0.034		400	73	36 [r]	s

a. Coercive force calculated as $2K/M_s$ for oriented samples, 0.96 $(K_1+K_2)/M_s$ for unoriented samples with uniaxial anisotropy, 0.64 K/M_s for unoriented samples with cubic anisotropy and [100] easy axis, 0.64 $[(4K_1/3)+(4K_2/9)]M_s$ for unoriented samples with cubic anisotropy and [111] easy axis.

b. H_{ci} measurements on unoriented samples designated by *r*.

c. A. Koch, P. Hokkeling, M. van der Steeg, and K. de Vos; "New Material for Permanent Magnets on a Base of Mn and Al," Journal Applied Physics 31, 75S (1960), doi:10.1063/1.1984610

d. C. Guillaud; thesis, University of Strashourg, 1943.

e. See Reference 9.

f. See Reference 8.

g. F. Pawlek and K. Reichel; Arch. Eisenhuttenwes 28, pp. 241 (1957).

h. W. Meiklejohn; "Experimental Study of the Coercive Force of Fine Particles," Review Modern Physics 25, pp. 302 (1953), doi:10.1103/RevModPhys.25.302

i. A. Berkowitz and W. Schuele; "Magnetic Properties of Some Ferrite Micropowders," Journal of Applied Physics 30, pp. 134S (1959), doi:10.1063/1.2185853

j. Fred Luborsky (unpublished results).

k. W. Johnston, R. Heikes, and J. Petrolo; "The Preparation of Fine Powder Hexagonal Fe_2C and its Coercive Force," Journal of Physical Chemistry 64, pp. 1720 (1960), doi:10.1021/j100840a028

l. C. Guillaud; Compt. Rend. 229, pp. 818 (1949).

m. W. Schuele; WADC Technical Report 58-136, April 1958.

n. G. van Oosterhout and C. Klomp; "On the effect of grinding upon the magnetic properties of magnetite and zinc ferrite," Applied Science Research 9, pp. 288 (1962), doi:10.1007/BF02921815

o. Fred Luborsky; "Comparison of the Size of Spherical Particles of Iron, Cobalt, and Alloys of Iron-Cobalt in Mercury as Determined by Various Methods," Journal of Applied Physics 33, pp. 1909 (1962), doi:10.1063/1.1728868

p. Louis Weil and Suzanne Marfoure; "Variation thermique du champ coercitif du nickel aggloméré," Journal Physics Radium 8, pp. 358 (1947), doi:10.1051/jphysrad:01947008012035800

q. W. Osmond; Proceedings Physics Society (London) A65, pp. 121 (1952); A66, pp. 265 (1953).

r. T. Sato, M. Sugihara, and M, Saito; Review Electrical Communications Laboratory 2, pp. 26, (1963).

Publishing History

First published in March 1966. Reformatted and color illustrations and updated references added by Mark Duncan in August 2009.

References

[1] For example, *Permanent Magnets and Magnetism*., edited by D. Hadfield (John Wiley & Sons, Inc., New York, 1962).

[2] K. J. de Vos; in Proceedings of the International Conference on Alagnetism, Nottingham, 1964 (The Institute of Physics and The Physical Society, London, 1965), p. 772.

[3] J. W. Cahn; "Magnetic Aging of Spinodal Alloys," Journal Applied Physics, Volume 34, pp. 3581 (1963), doi:10.1063/1.1729261

[4] T. O. Paine and Fred E. Luborsky; "'Interaction Anisotropy' Model of the Structure of Alnico Magnet Alloys," Journal of Applied Physics 31, pp. 785 (1960), doi:10.1063/1.1984611

[5] G. Begin and A. Dube; presented at 14th Canadian Metal Physics Conference, 1965.

[6] For a review, see Noboru Makino and Yasuo Kimura; "Techniques to Achieve Texture in Permanent Magnet Alloy Systems," Journal of Applied Physics 36,1185 (1965), doi:10.1063/1.1714162

[7] R. Wittig; Transactions of the First European Conference on Magnetism, Vienna, 1965, Volume 1, Paper 2.16.

[8] C. D. Mee and J. Jeschke; "Single-Domain Properties in Hexagonal Ferrites," Journal of Applied Physics 34, 1271 (1963), doi:10.1063/1.1729467

[9] K. Friess; Reference 7, Paper 2.12.

[10] Fred E. Luborsky; "Development of Elongated Particle Magnets," Journal of Applied Physics 32, 171S (1961), doi:10.1063/1.2000392; Journal Electrochemical Society 108, 1138 (1961).

[11] D. J. Craik and R. S. Tebble; "Magnetic domains," Report Progress Physics 24, 116 (1961), doi:10.1088/0034-4885/24/1/304

[12] Fred E. Luborsky; "Magnetization Reversal of Almost Perfect Whiskers," Journal of Applied Physics 35, 2055 (1964), doi:10.1063/1.1702791; Proceedings of the International Conference on Magnetism, Nottingham, 196-1 (The Institute of Physics and The Physical Society, London. 1965), p. 763.